Production and decay of the 125 GeV Higgs boson in the littlest Higgs model with T-parity[*]

ZENG Qing-Guo(曾庆国)[1,2]   YANG Shuo(杨硕)[3,4]   YUE Chong-Xing(岳崇兴)[1,1)]   CHEN Lian-Song(陈连松)[1]

[1] Department of Physics, Liaoning Normal University, Dalian 116029, China
[2] Department of Physics, Shangqiu Normal University, Shangqiu 476000, China
[3] Physics Department, Dalian University, Dalian 116622, China
[4] Center for High Energy Physics, Peking University, Beijing 100871, China

Abstract: Motivated by recent search results for the standard model (SM) Higgs boson at the Large Hadron Collider (LHC), we revisit the Higgs phenomenology in the littlest Higgs model with T-parity (LHT). We present the signal strength modifier μ, respectively, for the main search channels $qq' \to jjh \to jj\gamma\gamma$, $qq' \to Vh \to V\gamma\gamma$, $qq' \to Vh \to Vbb$, $gg \to h \to \gamma\gamma$, and $gg \to h \to VV$ in the LHT model. It is found that an enhancement factor of 1.09–1.56 in the $qq' \to jjh \to jj\gamma\gamma$ channel can be obtained for this model in Case B with parameter f in the range 500–1000 GeV. However, the rates for $b\bar{b}$, $\tau\bar{\tau}$ are significantly suppressed relative to the SM predictions, which are still consistent with the current sensitivity. It is hoped that this will be further tested with larger integrated luminosity at the LHC.

Key words: Higgs boson, Large Hadron Collider, littlest Higgs model with T-parity

PACS: 14.60.Hi, 12.60.-i, 13.66.De   **DOI:** 10.1088/1674-1137/37/5/054102

1 Introduction

The standard model (SM) is built on two cornerstones. One is gauge theory, which has been confirmed by the discovery of the electroweak gauge bosons W and Z and is further verified by electroweak precision measurements. However, the other one, the electroweak symmetry breaking (EWSB) mechanism, still requires a direct experimental test. The Large Hadron Collider (LHC) bears the responsibility for detecting the Higgs boson and revealing the mystery of EWSB.

Over a long period, the Higgs mass is a free parameter in a wide range from 114.4 to 700 GeV, which is based on the LEP search bound [1] and unitary constraint [2]. Lately, the Tevatron has excluded the production of a Higgs boson in the narrow mass window 156–177 GeV at 95% CL [3]. The LHC experiment has the potential to cover the Higgs boson search in the mass range from 100 GeV to TeV order. For a light Higgs with a mass below 120 GeV, the best search channel is h→γγ. At a medium mass range of 120–200 GeV, the best sensitivity is achieved in the WW channel. With the increase in the Higgs mass, the search channel h → ZZ → 4l and h→ZZ→2l2ν becomes more sensitive.

Recently, the ATLAS and CMS collaborations have released the search results for the SM Higgs based on the 2012 data corresponding to a luminosity of about 5–6 fb^{-1} at 8 TeV and the 2011 data around 5 fb^{-1} at the 7 TeV run [4, 5]. Both collaborations further confirmed the previous event excess [6, 7] and announced the discovery of a Higgs-like particle around 125 GeV with a local significance of the 5σ level.

It is interesting to note that the present Higgs search results from ATLAS and CMS still hint at a larger observed rate in h→γγ than the SM prediction, although this is not as evident as the previous results [4, 5, 8, 9]. Motivated by recent search results, especially the h→γγ excess, extensive studies have been carried out, including attempts to draw more information from the data and to use a global fit to get the best constraints on the Higgs effective couplings [10–12]. The global fit results show that the SM Higgs boson with a mass around 125 GeV can correctly predict the observed rates, but better fits are obtained by some non-standard scenarios that predict more γγ signal events [10–12].

In many new physics models, new particles are introduced and they will contribute significantly to Higgs production and decay. The current Higgs search results could provide clues into the underlying physics and then generate profound effects on new physics searches.

After the discovery of the Higgs-like boson, the next important mission is to test the properties of the particle, including its couplings to the SM particles and its spin and CP quantum numbers. Extensive studies on Higgs phenomena in different models are needed to verify, constrain or rule out different new physics models according to the data.

In the little Higgs models, new particles coupling to the Higgs boson are introduced to cancel the quadratic divergence of the Higgs mass induced by SM particles. Although no direct signal of little Higgs particles has been found until now, the search results for the Higgs boson can give important indirect constraints on these new particles and the model parameter space. The Higgs phenomenology in the littlest Higgs model with T-parity (LHT) [13] has been extensively studied in Refs. [14–16]. In this paper, we revisit the Higgs boson in the LHT model and test the parameter space in light of recent search data. We present the total width and the branching ratios for the Higgs boson with 125 GeV mass in the LHT model. It is expected that the width information of the Higgs boson in the LHT model could be further tested with a larger data sample. Furthermore, we study the search channels qq′ → jjh → jjγγ, qq′ → Vh followed by h→b$\bar{\rm b}$, gg→h→γγ, gg→h→WW, and gg→h→ZZ.

The rest of this paper is organized as follows. In Section 2, we briefly review the LHT model. In Section 3, we calculate the width information of the 125 GeV Higgs boson in the LHT model, and we also calculate the rates of the main Higgs search channels normalized to the SM prediction in the LHT model. Finally, we give our conclusions in Section 4.

2   The Higgs in the LHT model

A key feature of the little Higgs theory is that the Higgs boson is a pseudo-Goldstone boson from the breaking of a large global symmetry, and the EWSB is triggered by the Coleman-Weinberg potential [17]. In this paper, we shall focus on the LHT model, which has been the most popular little Higgs model in recent years. In the LHT model, a discrete parity called T-parity is introduced into the littlest Higgs model [18] and particle fields are divided into T-even and T-odd sectors under the parity, and the SM fields are T-even. Because all the dangerous tree-level contributions to low-energy EW observables are forbidden by T-parity, the relatively low symmetry breaking scale f is allowed.

To implement T-parity, two fermion $SU(2)$ doublets, q_1 and q_2 as $q_i = -\sigma_2(u_{{\rm L}_i}, d_{{\rm L}_i})^{\rm T} = -({\rm i}d_{{\rm L}_i}, -{\rm i}u_{{\rm L}_i})^{\rm T}$ with $i=1$ and 2, are introduced for each SM fermion doublet. q_1 and q_2 are embedded into incomplete $SU(5)$ multiplets Ψ_1 and Ψ_2 as $\Psi_1=(q_1, 0, 0_2)^{\rm T}$ and $\Psi_2=(0_2, 0, q_2)^{\rm T}$, where $0_2=(0, 0)^{\rm T}$. A multiplet $\Psi_{\rm c}$ is introduced as $\Psi_{\rm c}=(q_{\rm c}, \chi_{\rm c}, \tilde{q}_{\rm c})^{\rm T}$.

The fermion mass terms and interaction terms with the neutral Higgs boson are given by [13]

$$\mathcal{L}_\kappa = -\sqrt{2}\kappa f[\bar{d}_{{\rm L}_-}\tilde{d}_{\rm c}+\frac{1+c_\xi}{2}\bar{u}_{{\rm L}_-}\tilde{u}_{\rm c}$$

$$-\frac{s_\xi}{\sqrt{2}}\bar{u}_{{\rm L}_-}\chi_{\rm c}-\frac{1-c_\xi}{2}\bar{u}_{{\rm L}_-}u_{\rm c}]+{\rm h.c.}. \qquad (1)$$

$$\mathcal{L}_t = -\lambda_1 f\left(\frac{s_\Sigma}{\sqrt{2}}\bar{u}_{{\rm L}_+}u_{\rm R}+\frac{1+c_\Sigma}{2}\bar{U}_{{\rm L}_+}u_{\rm R}\right)$$

$$-\lambda_2 f\left(\bar{U}_{{\rm L}_+}U_{{\rm R}_+}+\bar{U}_{{\rm L}_-}U_{{\rm R}_-}\right)+{\rm h.c.}. \qquad (2)$$

Here,

$$c_\Sigma\left(\equiv\cos\frac{\sqrt{2}(v+h)}{f}\right)$$

and

$$s_\Sigma\left(\equiv\sin\frac{\sqrt{2}(v+h)}{f}\right)$$

originate from the non-linear sigma model field Σ. $u_{{\rm L}_-}$ and $u_{{\rm L}_+}$ are defined by $u_{{\rm L}_\pm} = (u_{{\rm L}_1}\mp u_{{\rm L}_2})/\sqrt{2}$ and they correspond to the T-odd and T-even eigenstates, respectively.

The T-odd combination of the doublets q_1 and q_2 obtain a mass $\sqrt{2}\kappa f$ from $\mathcal{L}_\kappa$ (cf. Eq. (1)). There are three generations of T-odd particles; here we assume they are degenerate. A T-odd Dirac Fermion T′ (T′$_{\rm L}$≡U$_{{\rm L}_-}$, T′$_{\rm R}$≡U$_{{\rm R}_-}$) gets a mass $m_{\rm T'}=\lambda_2 f$ (cf. Eq. (2)). Note that T′ does not have tree-level Higgs boson interaction, and thus it does not contribute to the gg fusion process at the one-loop order. The heavy T-even partner (T) of the top quark with the mass

$$m_T=\frac{m_{\rm t}}{\sqrt{x_{\rm L}(1-x_{\rm L})}}\frac{f}{\nu}$$

is responsible for canceling the quadratic divergence to the Higgs mass induced by the top quark where

$$x_{\rm L}=\frac{\lambda_1^2}{\lambda_1^2+\lambda_2^2}.$$

The effective Lagrangian for down-type quark Yukawa couplings in this paper is given by

$$\mathcal{L}_{\rm d} = \frac{{\rm i}\lambda_{\rm d}}{2\sqrt{2}}f\epsilon_{ij}\epsilon_{xyz}[(\bar{\Psi}_2')_x\Sigma_{iy}\Sigma_{jz}X$$

$$-(\bar{\Psi}_1'\Sigma_0)_x\tilde{\Sigma}_{iy}\tilde{\Sigma}_{jz}\tilde{X}]d_{\rm R}, \qquad (3)$$

where $\bar{\Psi}_1' = (-\sigma_2 q_1, 0, 0_2)^{\rm T}$ and $\bar{\Psi}_2' = (0_2, 0, -\sigma_2 q_2)^{\rm T}$. Here, X transforms into $\tilde{X}$ under T-parity, and $X = (\Sigma_{33})^{-\frac{1}{4}}$ (denoted as Case A) and $X=(\Sigma_{33}^\dagger)^{\frac{1}{4}}$ (denoted as Case B) are chosen for X. Here, Σ_{33} is the (3, 3) component of the non-linear sigma model field Σ.

In addition to new Higgs interactions introduced in the LHT model, the interactions between the Higgs boson and the SM particles are also modified as [14]:

$$\frac{g_{\mathrm{hVV}}}{g_{\mathrm{hVV}}^{\mathrm{SM}}} \approx 1-\frac{1}{4}\frac{v_{\mathrm{SM}}^2}{f^2}-\frac{1}{32}\frac{v_{\mathrm{SM}}^4}{f^4}, \quad (\mathrm{V=Z,W}), \qquad (4)$$

$$\frac{g_{\mathrm{hu\bar{u}}}}{g_{\mathrm{hu\bar{u}}}^{\mathrm{SM}}} \approx 1-\frac{3}{4}\frac{v_{\mathrm{SM}}^2}{f^2}-\frac{5}{32}\frac{v_{\mathrm{SM}}^4}{f^4} \quad (\mathrm{u=u, c}), \qquad (5)$$

$$\frac{g_{\mathrm{hd\bar{d}}}}{g_{\mathrm{hd\bar{d}}}^{\mathrm{SM}}} \approx 1-\frac{1}{4}\frac{v_{\mathrm{SM}}^2}{f^2}+\frac{7}{32}\frac{v_{\mathrm{SM}}^4}{f^4} \quad (\mathrm{Case\ A}), \qquad (6)$$

$$\frac{g_{\mathrm{hd\bar{d}}}}{g_{\mathrm{hd\bar{d}}}^{\mathrm{SM}}} \approx 1-\frac{5}{4}\frac{v_{\mathrm{SM}}^2}{f^2}-\frac{17}{32}\frac{v_{\mathrm{SM}}^4}{f^4} \quad (\mathrm{Case\ B}). \qquad (7)$$

The relation of lepton Yukawa couplings are the same as the down-type Yukawa couplings.

3   Numerical results and analysis

In this paper, instead of studies of all the search channels, we mainly concentrate on five channels: vector boson fusion (VBF) followed by di-photon decay, i.e. $qq' \to jjh \to jj\gamma\gamma$, $qq' \to Vh$ followed by $h \to b\bar{b}$, $gg \to h \to \gamma\gamma$, $gg \to h \to WW$, and $gg \to h \to ZZ$. This is because among all the search channels, these five channels provide a crucial role due to the large event rates and good reconstructed resolution. In the LHT model, the additional T-even top partner and the T-odd fermions contribute significantly to the processes $gg\to h$ and $h\to\gamma\gamma$ induced at loop level. Modified couplings of the SM particles as shown in Eqs. (4)–(7) also affect the production rates and decay widths of h.

In our calculation, the gg fusion process is calculated by private codes using the loop functions, and VBF and Vh production processes are calculated with Madgraph4 [19], where the parton distribution function CTEQ6L [20] is used with the renormalization scale μ_{R}, and the factorization scale μ_{F} is chosen to be $\mu_{\mathrm{R}}=\mu_{\mathrm{F}}=m_{\mathrm{h}}$. The Higgs decays are calculated with HDECAY [21].

In the LHT model, the loop-induced partial decay width of $h\to\gamma\gamma$[1]) can be represented as

$$\Gamma(\mathrm{H}\to\gamma\gamma)=\frac{\sqrt{2}G_{\mathrm{F}}\alpha^2 m_{\mathrm{H}}^3}{256\pi^3}\left|\frac{4}{3}F_{1/2}(\tau_t)y_t y_{G_{\mathrm{F}}}\right.$$

$$+\frac{4}{3}F_{1/2}(\tau_{\mathrm{T}})y_{\mathrm{T}}+\frac{4}{3}F_{1/2}(\tau_{\mathrm{T}'})y_{\mathrm{T}'}$$

$$\left.+F_1(\tau_{\mathrm{W_L}})y_{\mathrm{W_L}}y_{G_{\mathrm{F}}}+F_1(\tau_{\mathrm{W_H}})y_{\mathrm{W_H}}\right|^2, \qquad (8)$$

where y_{i} represents the corresponding Higgs coupling in the LHT model. T, T' and W$_{\mathrm{H}}$ represent, respectively, the T-even top partner, T-odd fermions and heavy charged gauge bosons in the model. Here, the dimension-

less loop factors [23] are

$$F_1=2+3\tau+3\tau(2-\tau)f(\tau),$$

$$F_{1/2}=-2\tau[1+(1-\tau)f(\tau)],$$

$$F_0=\tau[1-\tau f(\tau)], \qquad (9)$$

with

$$f(\tau)=\begin{cases}\left[\sin^{-1}(1/\sqrt{\tau})\right]^2, & \tau\geqslant 1 \\ -\frac{1}{4}[\ln(\eta_+/\eta_-)-\mathrm{i}\pi]^2, & \tau<1\end{cases} \qquad (10)$$

and

$$\tau_{\mathrm{i}}=4M_{\mathrm{i}}^2/m_{\mathrm{H}}^2, \quad \eta_\pm=1\pm\sqrt{1-\tau}. \qquad (11)$$

For the $h \to gg$ process, the contributions from the T-even top partner and T-odd fermions significantly suppress its rate because in little Higgs models, the quadratic contribution to the Higgs mass from the top quark is canceled by the contribution from its partner, which is derived from the underlying collective symmetry breaking. For the $h\to\gamma\gamma$ decay, the W boson contribution dominates over the top contribution in the SM and they will partially cancel. The contributions from additional fermions tend to cancel the contributions from new gauge bosons, and the W boson still gives a dominant contribution. Therefore, the partial decay width of $h\to\gamma\gamma$ does not vary much. However, the branching ratio of $h\to\gamma\gamma$ is enhanced significantly due to total width suppression in Case B. For precision, we have included all the new particle contributions in the loop. Our numerical calculation shows that the decay $h\to\gamma\gamma$ and the production process $gg \to h$ are not sensitive to the free parameters x_{L} and κ. Thus, in this paper, we fix $x_{\mathrm{L}}=0.5$ and $\kappa=1$

We first present the values of the total width and branching ratios for two typical values, $f=800$ GeV and $f = 1000$ GeV, in Table 1, and it is expected that the width information of the Higgs in the LHT model could be further tested at the LHC. For the SM Higgs boson with a light mass of 125 GeV, the $b\bar{b}$ channel is the dominant decay channel and the total width of the SM Higgs boson is about 4.03 MeV [24]. When it comes to the Higgs boson in the LHT model, the dominant channel is still the $h\to b\bar{b}$. However, there are some differences.

In both Case A and Case B, the total widths of the Higgs boson are suppressed. In Case A, the main decay channels of $b\bar{b}$, $\tau\bar{\tau}$, VV are slightly suppressed in similar factors because the corresponding couplings are suppressed, as shown in Eqs. (4)–(7). While in Case B, the b and τ Yukawa couplings are significantly suppressed. For the Higgs with mass 125 GeV, the $b\bar{b}$ and $\tau\bar{\tau}$ channels are the dominant decay channels. Hence, the suppression of the Yukawa couplings of $hb\bar{b}$ and $h\tau\bar{\tau}$

---

1) A detailed study of loop-induced decay in the littlest Higgs model can be found in Ref. [22].

Table 1.   Higgs branching ratios and total widths in the LHT model. (m_h=125 GeV).

f/GeV(Case)	$b\bar{b}$	$\tau\bar{\tau}$	$c\bar{c}$	$s\bar{s}$	$\mu\mu$	gg
800 (A)	0.5922	0.6489E−01	0.2688E−01	0.4508E−03	0.2252E−03	0.6221E−01
1000 (A)	0.5857	0.6419E−01	0.2770E−01	0.4457E−03	0.2227E−03	0.7065E−01
800 (B)	0.5461	0.5984E−01	0.3084E−01	0.4162E−03	0.2076E−03	0.7229E−01
1000 (B)	0.5578	0.6112E−01	0.3012E−01	0.4246E−03	0.2121E−03	0.7740E−01

f/GeV(Case)	$\gamma\gamma$	zγ	ww	zz	$t\bar{t}$	total Γ_h/GeV
800 (A)	0.2383E−02	0.1651E−02	0.2215	0.2712E−01	0	0.379332E−02
1000 (A)	0.2341E−02	0.1609E−02	0.2197	0.2689E−01	0	0.389284E−02
800 (B)	0.2734E−02	0.1894E−02	0.2541	0.3111E−01	0	0.330616E−02
1000 (B)	0.2546E−02	0.1749E−02	0.2389	0.2925E−01	0	0.357995E−02

results in the evident reduction in the total width of the Higgs boson. However, it is interesting to note that this also leads to an enhancement of the branching ratio of h→γγ. The suppression factor of the branching ratios of h→b$\bar{\text{b}}$ and hτ$\bar{\tau}$, and the enhancement factor of the branching ratio of h→γγ, can be read directly from the table.

Here, we also present the total decay width of the Higgs boson in the LHT model normalized to the SM width as a function of f in Fig. 1. As shown in Fig. 1, in both Case A and Case B, the total widths are suppressed in the whole f range. When f increases, the decoupling effect appears and the ratio is close to one. The suppression factors are about 0.838–0.988 (Case A), and 0.543–0.967 (Case B) for f in the range 500–2000 GeV, respectively. As stated above, the suppression of the total widths is derived from the suppressions of the Higgs couplings in the LHT model. In particular, the total widths are significantly suppressed in Case B since the suppression of the Yukawa couplings of hb$\bar{\text{b}}$ directly affects the dominant decay channel h→b$\bar{\text{b}}$.
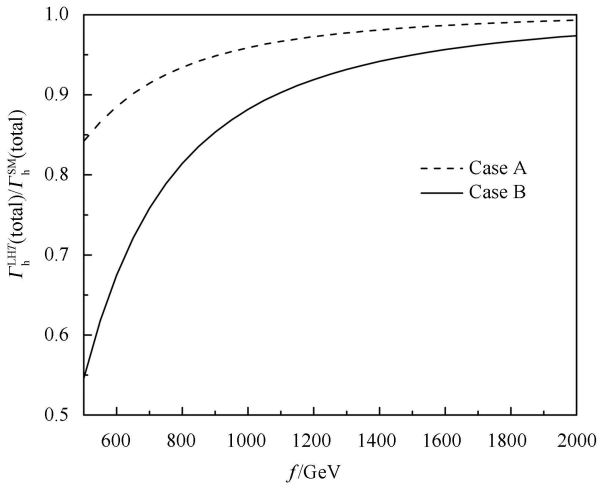

Fig. 1. Γ_h^{LHT}(total)/Γ_h^{SM}(total) as a function of scale parameter f.

Furthermore, we also calculate the hadron production cross sections for the gluon-gluon fusion process gg→h,

the vector-boson fusion process qq′→jjh, the associated Higgs production with W/Z, qq′→Wh and q$\bar{\text{q}}$→Zh at the LHC. Both cases corresponding to $\sqrt{s}$=7 TeV and $\sqrt{s}$=8 TeV are considered, and the results are shown in Fig. 2. Here, we mainly focus on the case for the 125 GeV Higgs and our results are consistent with those results. As shown in Fig. 2, in the low f range, the cross section for gluon-gluon fusion is significantly suppressed as interpreted above, and the other modes are also suppressed because of the modified couplings in the LHT model. When f increases, the cross section is close to the SM prediction. From a phenomenological point, the difference between Case A and Case B is the coupling of hd$\bar{\text{d}}$, where d represents the down-type fermions. So the cross sections shown in Fig. 2 are the same for Case A and Case B.
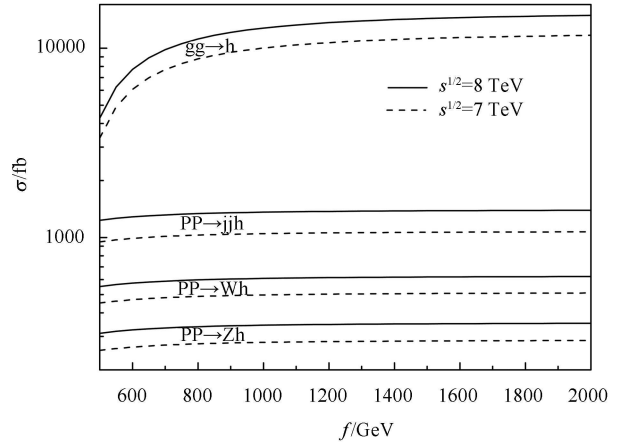

Fig. 2.   The cross sections for the main modes of Higgs production in the LHT model as a function of scale parameter f.

Here, we further consider the signal strength modifier $\mu_i = \dfrac{\sigma(\mathrm{LHT})\times Br_i(\mathrm{LHT})}{\sigma(\mathrm{SM})\times Br_i(\mathrm{SM})}$. In Figs. 3–6, taking m_h=125 GeV, we show $\mu_{\gamma\gamma jj}$, μ_{Vbb}, $\mu_{\gamma\gamma}$, μ_{VV} (V=W,Z) versus the parameter f, respectively, for the production channels qq′→hjj→γγjj, qq′→Vh→Vbb, gg→h→γγ, gg→h→VV in Case A and Case B.
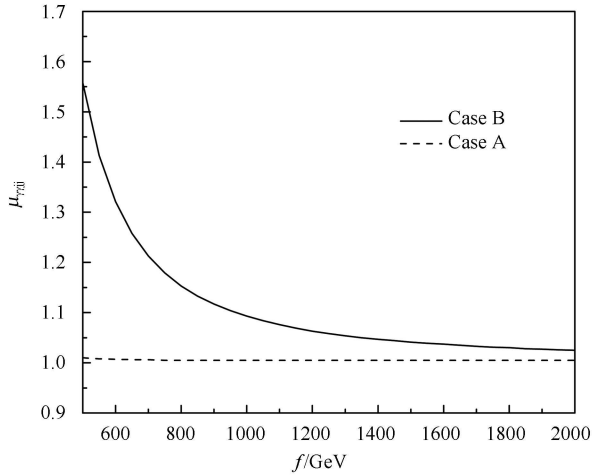
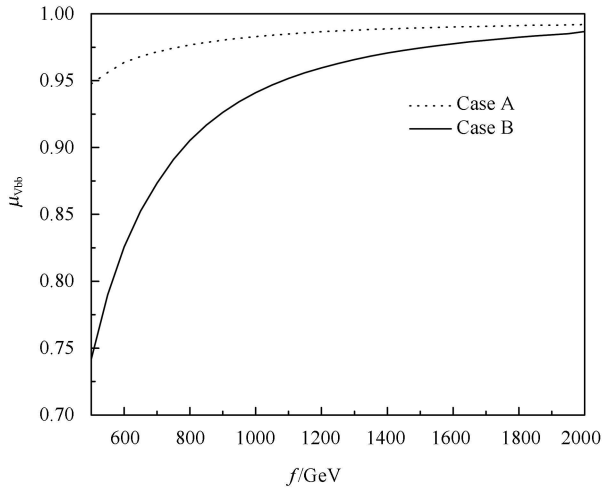Fig. 3.   The $\mu_{\gamma\gamma jj}(qq' \to jjh \to jj\gamma\gamma)$ rates as a function of scale parameter f.

Fig. 4.   The $\mu_{Vbb}(qq' \to Vh \to Vb\bar{b})$ rates as a function of scale parameter f.

It is found that $\mu_{\gamma\gamma jj}$ corresponding to the vector-boson fusion production followed by di-photon decay is larger than one in the small f region in Case B, as shown in Fig. 3. This was also noted in Ref. [14]. This is mainly because in Case B, both $h \to b\bar{b}$ and $h \to \tau\bar{\tau}$ are significantly suppressed due to the shift in the couplings (as shown in Eq. (7)), which induces the branching ratios of $h \to \gamma\gamma$ to increase. The increase effects dominate over the reduced effects in production. The signal strength $\mu_{\gamma\gamma jj}$ normalized to the SM prediction can reach 1.09–1.56 for parameter f in the range 500–1000 GeV. The hint of enhanced photon production rate in the vector boson fusion process [9] can be interpreted as the effect of small f in Case B of the LHT model. The ratio for channel $qq' \to Vh \to \gamma\gamma$ is nearly the same as $\mu_{\gamma\gamma jj}$ because they mainly depend on the VVh coupling and the

branching ratio of $h \to \gamma\gamma$. However, the $\gamma\gamma$ enhancement can not be interpreted in Case A. If more data are collected and it is further verified that events in the $\gamma\gamma jj$ channel are indeed larger than the SM prediction, then Case A will be ruled out and Case B will suffer further tests.

The $\mu_{\gamma\gamma}$ and μ_{VV} rates as a function of f are also illustrated in Figs. 5–6. The ratios $\mu_{\gamma\gamma}$ and μ_{VV} are suppressed in both Case A and Case B because the gluon-gluon fusion process is significantly suppressed by the contributions from additional heavy fermions. The cross section for subprocess $gg \to h$ can be represented as

$$\hat{\sigma}(gg \to h) = \Gamma(h \to gg)\frac{\pi^2}{8m_h^3}. \qquad (12)$$

Both the T-even top partner and extra T-odd fermions are considered in the loop calculation. The effective tree level approximation in the so-called heavy top limit is not used[1]. The deviations from the SM prediction for $\mu_{\gamma\gamma}$ and μ_{VV} are sensitive to the parameter f. When f increases, the suppression is weakened sharply and the results are close to the SM predictions in the decoupling limit. Besides, the rate $\mu_{\gamma\gamma}$ for Case B is larger than that for Case A. The main reason for this is that the large shift in hb$\bar{b}$ coupling induces the significant increase of the branching ratio $Br(h \to \gamma\gamma)$. A similar conclusion of the deviation also holds for μ_{VV} in Fig. 6. Our results are consistent with those in Refs. [14–16].
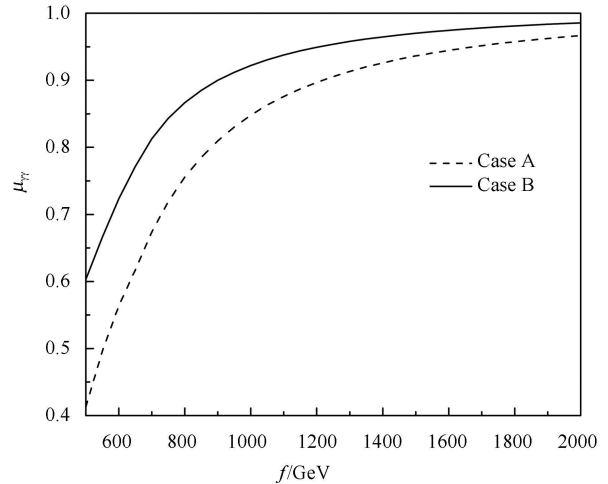

Fig. 5.   The $\mu_{\gamma\gamma}(gg \to h \to \gamma\gamma)$ rates as a function of the scale parameter f.

As shown above, an enhancement factor of 1.09–1.56 in the $qq' \to jjh \to jj\gamma\gamma$ channel can be obtained for the LHT model in Case B with parameter f in the range 500–1000 GeV. And in the same region, the event rates

---

1) There are detailed discussions about the comparison between loop calculation and heavy top approximation for the gluon-gluon fusion process in Refs. [25, 26].
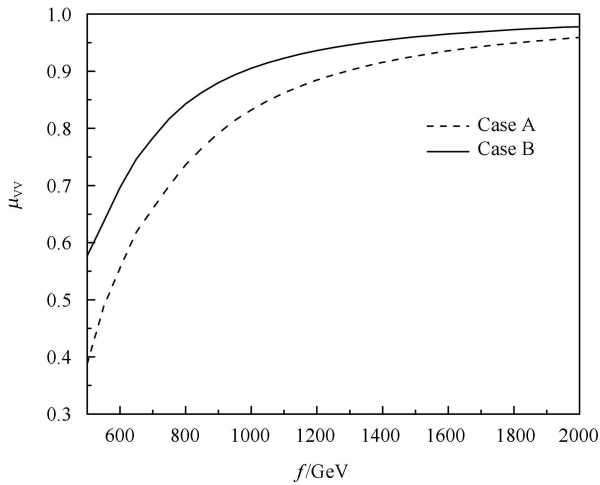
Fig. 6.   The $\mu_{VV}(gg \to h \to VV)$ rates as a function of scale parameter f.

in the WW and ZZ channels are slightly suppressed. Although the $h \to b\bar{b}$ and $h \to \tau\bar{\tau}$ are significantly suppressed, these two channels are not sensitive due to the large backgrounds and relative low identification efficiencies of the final states. In addition, the Higgs have not been conclusively observed in these two channels. So the Higgs boson of the LHT model in Case B with a small f value could fit well with the current Higgs search data. In Ref. [11], they got a 90% CL favored region corresponding to low mass m_T in the toy LHT model[1]. Based on the above calculation and analysis, we conclude that the current Higgs search result favors the LHT model in Case B with a low scale parameter f. The study in the framework of varying Yukawa couplings [27] also supports this conclusion. It is expected that the Higgs sector of the LHT model could be further tested by the LHC by increasing the integrated luminosity.

4   Conclusions

In both ATLAS and CMS analyses, the decay channel $h \to \gamma\gamma$ has played an important role in discovering the Higgs boson. Motivated by the recent results from the Higgs search at the LHC, extensive studies have been conducted to accommodate the hint of $h \to \gamma\gamma$ enhancement [10–12, 27–32]. In general, the enhancement factor in $h \to \gamma\gamma$ can be obtained via the contributions from new particles in the loop of $h \to \gamma\gamma$ or by suppressing the Yukawa couplings in the fermion sector. For the supersymmetric (SUSY) models, the h$\gamma\gamma$ can be enhanced by the contribution of $\tilde{\tau}$. A comparative study on different SUSY models was carried out in Ref. [28]. This shows that the most favored SUSY model is the next-to-minimal supersymmetric model (NMSSM), whose predictions about the 125 GeV Higgs boson can agree with the experimental data at the 1σ level without any fine tuning [28], while the minimal supersymmetric standard model (MSSM) suffers from some fine tuning [28]. Ref. [29] shows that the 125 GeV techni-dilaton in the walking technicolor (WTC) can be consistent with the current Higgs search results, where a large diphoton event rate can be achieved due to the loop contributions of extra techni-fermions. In addition, the minimal model of universal extra dimensions (MUED) explains how the cross-sections for Higgs production via gluon fusion and decay into photons are modified by KK particles running in loops [30]. On the other hand, in some other studies, the enhancement factor in $h \to \gamma\gamma$ can be obtained by modifying the Yukawa couplings [27, 32].

In this paper, we have studied the Higgs production and decay of the LHT model in the light of recent Higgs searches at ATLAS and CMS. The decay channels and cross sections for the 125 GeV Higgs boson in the LHT model are presented. We found that the total widths are suppressed in both Case A and Case B of the LHT model. However, the branching ratios of $h \to \gamma\gamma$ are enhanced in Case B in the small f region since the main decay channel $h \to b\bar{b}$ is significantly suppressed. The signal rates normalized to the SM prediction for Higgs ($m_h = 125$ GeV) search channels $qq' \to jjh \to jj\gamma\gamma$, $qq' \to Vh \to Vb\bar{b}$, $gg \to \gamma\gamma$, $gg \to WW$, $gg \to ZZ$ are also presented. It is found that an enhancement factor of 1.09–1.56 in the $qq' \to jjh \to jj\gamma\gamma$ channel can be obtained for the LHT model in Case B with parameter f in the range 500–1000 GeV. In the LHT model, the rates for $b\bar{b}$, $\tau\bar{\tau}$ in Case B are significantly suppressed relative to the SM predictions that are still consistent with the current statistic. It is expected that the Higgs properties of the LHT model could be further tested with a larger data sample at the LHC.

---

1) Their study was carried out in the fermionic top partner frame and only the most basic features of the LHT model are kept under some assumptions. In particular, the hVV couplings and hbb couplings are assumed to be consistent with those in the SM.

References

1 Barate R et al. (LEP Working Group for Higgs boson searches and ALEPH and DELPHI and L3 and OPAL Collaborations). Phys. Lett. B, 2003, **565**: 61–75

2 Marciano W J, Willenbrock S. Phys. Rev. D, 1998, **37**: 2509; Dawson S, Willenbrock S. Phys. Rev. Lett., 1989, **62**: 1232

3 Aaltonen T et al. (CDF and D0 collaboration). Phys. Rev. Lett., 2010, **104**: 061802; [TEVNPH (Tevatron New Phenomina and Higgs Working Group) and CDF and D0 collaborations]. arXiv:1107.5518

4 Gianotti F (the ATLAS collaboration). Talk given at CERN on July 4, 2012

5 Incandela J (the CMS collaboration). Talk given at CERN on July 4, 2012

6 Aad G et al. (ATLAS collaboration). Phys. Lett. B, 2012, **710**: 49–66

7 Chatrchyan S et al. (CMS collaboration). Phys. Lett. B, 2012, **710**: 26–48

8 Aad G et al. (ATLAS collaboration). Phys. Rev. Lett., 2010, **108**: 111803

9 Chatrchyan S et al. (CMS collaboration). Phys. Lett. B, 2012, **710**: 403–425

10 Azatov A, Contino R, Galloway J. JHEP, 2012, **1204**: 127

11 Carmi D, Falkowski A, Kuflik E, Volansky T. JHEP, 2012, **1207**: 136

12 Espinosa J R, Grojean C, Muhlleitner M, Trott M. JHEP, 2012, **1205**: 097; Giardino P P, Kannike K, Raidal M, Strumia A. JHEP, 2012, **1206**: 117; Carmi D, Falkowski A, Kuflik E, Volansky T, Zupan J. arXiv:1207.1718

13 Cheng H C, Low I. JHEP, 2003, **0309**: 051; JHEP, 2004, **0408**: 061; Low I. JHEP, 2004, **0410**: 067; Hubisz J, Meade P. Phys. Rev. D, 2005, **71**: 035016; Hubisz J, Meade P, Noble A, Perelstein M. JHEP, 2006, **0601**: 135

14 CHEN C R, Tobe K, YUAN C P. Phys. Lett. B, 2006, **640**: 263–271

15 WANG L, YANG J M. Phys. Rev. D, 2009, **79**: 055013

16 WANG L, YANG J M. Phys. Rev. D, 2011, **84**: 075024

17 Arkani-Hamed N, Cohen A G, Georgi H. Phys. Lett. B, 2001, **513**: 232-240; Arkani-Hamed N, Cohen A G, Katz E, Nelson A E, Gregoire T, Wacker J G. JHEP, 2002, **0208**: 021; Schmaltz M, Tucker-Smith D. Ann. ReV. Nucl. Part. Sci, 2005, **55**: 229

18 Arkani-Hamed N, Cohen A G, Katz E, Nelson A E. JHEP, 2002, **0207**: 034

19 Maltoni F, Stelzer T. JHEP, 2003, **0302**: 027

20 Pumplin J et al. JHEP, 2006, **0602**: 032

21 Djouadi A, Kalinowski J, Spira M. Comput. Phys. Commun, 1998, **108**: 56–74

22 HAN T, Logan H E, McElrath B, WANG L T. Phys. Lett. B, 2003, **563**: 191–202

23 Gunion J F, Haber H E, Kane J L, Dawson S. The Higgs Hunter's Guide, Addison-Wesley, Reading, MA (1990)

24 Dittmaier S et al. (LHC Higgs Cross Section Working Group collaboration). Handbook of LHC Higgs Cross Sections: 1. Inclusive Observables. arXiv:1101.0593

25 Barger V, Philips R. Collider Physics, Redwood City: Addison-Wesley Publishing Company, 1988

26 LIU C, YANG S. Phys. Rev. D, 2010, **81**: 093009

27 LI T J, WAN X, WANG Y K, ZHU S H. JHEP, 2012, **1209**: 086. arxiv:1203.5083

28 CAO J J, HENG Z X, YANG J M, ZHU J Y. arXiv:1207.3698

29 Matsuzaki S, Yamawaki K. arXiv:1207.5911; Matsuzaki S, Yamawaki K. Phys. Rev. D, 2012, **86**: 035025. arxiv:1206.6703

30 Belanger G, Belyaev A, Brown M, Kakizaki M, Pukhov A. EPJ Web Conf., 2012, 28: 12070

31 Arhrib A, Benbrik R, Chabab M, Moultaka G, Rahili L. JHEP, 2012, **1204**: 136; Kanemura S, Yagyu K. Phys. Rev. D, 2012, **85**: 115009; CAI Y, CHAO W, YANG S. arXiv:1208.3949

32 Blum K, D'Agnolo R. Phys. Lett. B, 2012, **714**: 66–69